



Published in final edited form as:

*J Proteome Res.* 2017 April 07; 16(4): 1763–1772. doi:10.1021/acs.jproteome.7b00024.

## Quantitative Proteomic Analysis of Serum Exosomes from Patients with Locally Advanced Pancreatic Cancer Undergoing Chemoradiotherapy

Mingrui An<sup>†,§</sup>, Ines Lohse<sup>‡,§</sup>, Zhijing Tan<sup>†</sup>, Jianhui Zhu<sup>†</sup>, Jing Wu<sup>†</sup>, Himabindu Kurapati<sup>‡</sup>, Meredith A. Morgan<sup>‡</sup>, Theodore S. Lawrence<sup>‡</sup>, Kyle C. Cuneo<sup>\*,‡</sup>, and David M. Lubman<sup>\*,†</sup>

<sup>†</sup>Department of Surgery, University of Michigan Medical Center, Ann Arbor, Michigan 48109, United States

<sup>‡</sup>Department of Radiation Oncology, University of Michigan, Ann Arbor, Michigan 48109, United States

### Abstract

Pancreatic cancer is the third leading cause of cancer-related death in the USA. Despite extensive research, minimal improvements in patient outcomes have been achieved. Early identification of treatment response and metastasis would be valuable to determine the appropriate therapeutic course for patients. In this work, we isolated exosomes from the serum of 10 patients with locally advanced pancreatic cancer at serial time points over a course of therapy, and quantitative analysis was performed using the iTRAQ method. We detected approximately 700–800 exosomal proteins per sample, several of which have been implicated in metastasis and treatment resistance. We compared the exosomal proteome of patients at different time points during treatment to healthy controls and identified eight proteins that show global treatment-specific changes. We then tested the effect of patient-derived exosomes on the migration of tumor cells and found that patient-derived exosomes, but not healthy controls, induce cell migration, supporting their role in metastasis. Our data show that exosomes can be reliably extracted from patient serum and analyzed for protein content. The differential loading of exosomes during a course of therapy suggests that exosomes may provide novel insights into the development of treatment resistance and metastasis.

### Graphical abstract

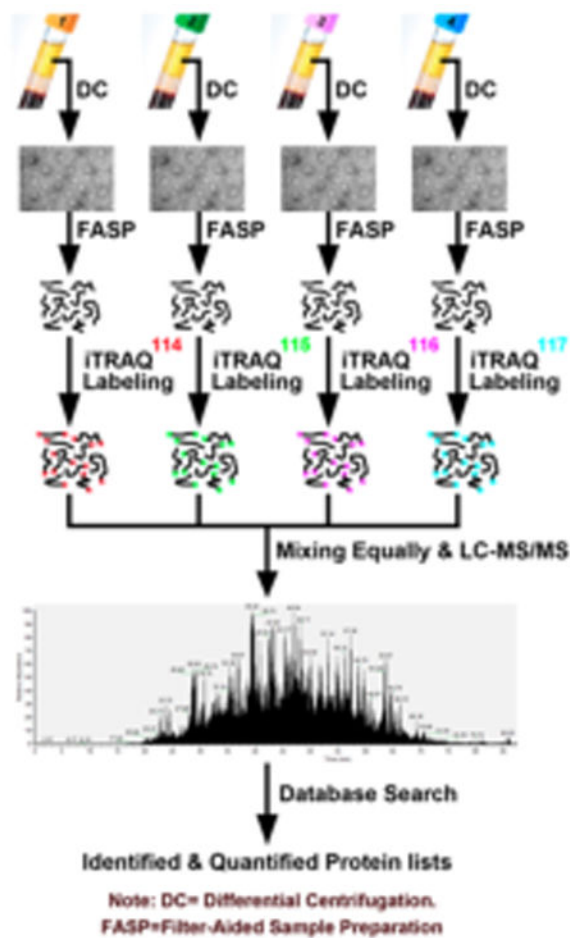
\*Corresponding Authors: K.C.C: Phone: (734)-936-4300. Fax: (734)-763-7370. kcuneo@umich.edu; D.M.L.: Phone: (734)-615-5081. Fax: (734)-615-2088. dmlubman@umich.edu.

§**Author Contributions:** M.A and I.L. authors contributed equally to this work

Supporting Information: The Supporting Information is available free of charge on the ACS Publications website at DOI: 10.1021/acs.jproteome.7b00024.

**ORCID:** David M. Lubman: 0000-0001-7731-0232

**Notes:** The authors declare no competing financial interest.



## Keywords

pancreatic cancer; exosomes; iTRAQ; chemotherapy; chemoradiation; metastasis

## Introduction

Pancreatic cancer is the third leading cause of cancer-related death in the USA, with a 5 year survival rate of <5%.<sup>1</sup> The poor prognosis of pancreatic cancer patients can be attributed to the biologically aggressive nature of these tumors combined with late clinical presentation. While surgical removal of the tumor represents the best treatment option for pancreatic cancer patients, only 20% of patients qualify for surgery. The majority of patients present with unresectable locally advanced or metastatic disease which contributes to the dismal prognosis of pancreatic cancer patients. Chemotherapy or chemoradiotherapy is typically offered to patients with locally advanced disease.<sup>2,3</sup>

Because of the lack of serial biopsies and clinically available blood biomarkers, the early assessment of treatment response and detection of metastatic disease remains a major challenge in the management of pancreatic cancer.<sup>4</sup> Early identification of treatment responses would help select the most appropriate therapeutic approach and limit treatment-

related toxicity in nonresponding patients. Several studies have examined molecular biomarkers in pancreatic cancer over the past decade; however, very few of the proposed markers have shown clinical relevance.<sup>5,6</sup> Thus novel biomarkers of early treatment response, tumor progression, and metastasis are greatly needed to improve the outcome of patients with locally advanced pancreatic cancer.<sup>7,8</sup>

Obtaining serial tissue biopsies over the course of treatment is not feasible in pancreatic cancer patients due to the invasive nature and risks associated with a biopsy, whereas serum exosomes can be safely and easily obtained at any time point as part of routine blood draws. Exosomes are a type of nanosized membrane-derived vesicle secreted by cells.<sup>9–12</sup> Exosomes are specifically loaded with cargo proteins and functional RNA molecules<sup>12–15</sup> and released into the extracellular space upon fusion with the plasma membrane. Their secretion has been observed from all types of normal and tumor cells, where they carry various cellular proteins throughout the body and act as a means of intercellular communication to transport signals to other organs.<sup>12,16,17</sup> As a result of their formation from the plasma membrane, there are many cell surface membrane proteins that can be detected in exosomes, some of which are diagnostic of the presence of cancer.<sup>18</sup> Thus exosomes have been identified as a potential tool to monitor response to cancer therapy.<sup>11,18–20</sup>

Tumor-derived exosomes contain tumor-related antigens and cancer-specific surface markers among other cargo. Changes in surface markers and exosomal cargo over the course of therapy may provide predictive and prognostic information that can be used to stratify patients for specific therapeutic approaches. In diseases such as glioblastoma, exosomes have shown promise as predictive biomarkers based on the detection of several proteins, most notably EGFR.<sup>20</sup> Tumor-derived exosomes can be isolated from patients using a number of different techniques including affinity enrichment and ultracentrifugation and thus can provide a minimally invasive method for therapeutic monitoring.<sup>21–24</sup>

Previous studies on serum exosomes could only identify several hundred proteins and thus might have failed to detect low-abundance proteins that may be relevant for their role in cancer.<sup>20,25,26</sup> These studies on tumor-derived exosomes were only able to detect and quantify a small number of high-abundance proteins and thus may have failed to detect biologically relevant changes. Moreover, a lack of appropriate quantification methods for serum-derived exosomal proteins does not allow for the reliable comparison of exosomal cargo from multiple samples from the same patient or between different patients.

This work aims to overcome the current limitations. We isolated exosomes from the serum of locally advanced pancreatic cancer patients using five cycles of ultracentrifugation. The samples included a mix of healthy serum controls and serum of patients with pancreatic cancer before treatment, after chemotherapy, and at the midpoint of chemoradiotherapy. The iTRAQ-based quantification method was optimized to increase the quantification accuracy and the number of proteins that were identified and quantified. Our goal was to use this method to quantitatively evaluate short-term changes in exosome protein expression and potential biomarkers in response to treatment.

## Materials and Methods

### Serum Samples

Serum samples of healthy subjects (Innovative Research, Novi, MI) were used as the control. Serum samples from a cohort of patients ( $n = 10$ ) with locally advanced pancreatic cancer (T4N0-1M0) undergoing chemoradiotherapy were obtained as part of an Institutional Review Board approved protocol (HUM00085016) at set time points during a course of therapy. Blood samples were obtained prior to treatment (T1), after 3 weeks of induction gemcitabine-based chemotherapy (T2), and at the midpoint of chemoradiotherapy (3 weeks into a 5 week course) (T3). Whole blood samples were centrifuged to separate out serum. All serum samples were stored at  $-80\text{ }^{\circ}\text{C}$  until analysis.

All patients received gemcitabine in combination with the Wee1 inhibitor (AZD1775) and chemoradiation therapy as part of a prospective phase I study. Gemcitabine was administered intravenously on days 1 and 8 of a 3 week cycle at a dose of  $1000\text{ mg/m}^2$ . AZD1775 was given orally on days 1, 2, and 8, 9 of each 3 week cycle. Radiation was delivered concurrently with cycles 2 and 3. All patients received  $52.5\text{Gy}$  in 25 daily fractions over 5 weeks to the primary tumor using volumetric modulated radiation therapy to spare normal tissue.

### Isolation of Exosomes from Human Serum

The initial volume of serum for the experiments was 4 mL per sample. The samples were diluted with an equal volume of PBS (AppliChem, St. Louis, MO) to decrease the viscosity. The diluted serum samples were centrifuged at  $2000g$  for 10 min and  $10\ 000g$  for 30 min at  $4\text{ }^{\circ}\text{C}$  to remove dead cells and cell debris. The supernatant was transferred into Ultra-Clear™ tubes (Beckman Coulter, Indianapolis, IN) and centrifuged at  $100\ 000g$  using a Beckman Optima XL-70 ultracentrifuge for 70 min at  $4\text{ }^{\circ}\text{C}$ . The supernatant was removed with a pipet, and 2 mm of supernatant remained above the pellet. After one cycle of ultracentrifugation, it was not possible to remove all of the serum supernatant, where  $\sim 2\text{ mm}$  of supernatant at the bottom was left to avoid the loss of exosome sediment. Five cycles of ultracentrifugation were necessary to purify exosomes and remove serum proteins including albumin.<sup>27</sup> The exosomes were suspended in 4 mL of PBS and centrifuged at  $100\ 000g$  for 60 min at  $4\text{ }^{\circ}\text{C}$  to clean the exosomes. This cleanup step was repeated three additional times.

### Western Blot

Exosome protein ( $\sim 0.2\ \mu\text{g}$ ) from 4 mL of serum was separated on a 4–15% SDS-PAGE gradient gel (Bio-Rad, Berkeley, CA) and transferred to a PVDF membrane (Bio-Rad, Berkeley, CA). After blocking, the membrane was incubated overnight with anti-CD63 antibody (1:200, no. 10630D, Abcam, San Francisco, CA), followed by incubation with HRP-conjugated antirabbit antibody (Jackson ImmunoResearch, West Grove, PA), and was visualized using a chemiluminescent method kit (Merck Millipore, Billerica, MA).

### Lysis of Exosomes, Tryptic Digestion, and iTRAQ Labeling

After removing the supernatant, exosomes were lysed with  $25\ \mu\text{L}$  of lysis buffer composed of 50 mM triethylammonium bicarbonate (TEAB), 4% SDS, and 100 mM 1,4-dithiothreitol

at 99 °C for 5 min. The sample was cooled down, and 25  $\mu\text{L}$  of 250 mM of iodoacetamide was added and then diluted with 1 mL of 8 M urea buffer (containing 50 mM TEAB). Next, the filter-aided sample preparation (FASP) method was performed. The sample solution was transferred to a centrifugal spin YM-30 filter (Millipore, Billerica, MA), and centrifuged at 14 000g for 20 min. Then, 200  $\mu\text{L}$  of 8 M urea was added to wash the sample with the same centrifugation condition three times. To remove the urea buffer, the sample was washed with 200  $\mu\text{L}$  of 50 mM TEAB also with this centrifugation condition three times. The samples ( $\sim 0.2$  to  $0.6 \mu\text{g}$ ) were then digested by 200 ng sequencing-grade modified trypsin (Promega, Fitchburg, WI) at 37 °C overnight. The tryptic digest was collected by centrifugation. The samples were acidified and desalted using a  $\text{C}_{18}$  tip. The eluted samples were dried by SpeedVac (Labconco, Kansas City, MO).

Peptide samples from the standard serum ( $\sim 0.6 \mu\text{g}$ ) and three time points of patient serum ( $\sim 0.2 \mu\text{g}$ ) were labeled by 4-plex iTRAQ reagent (tag mass: 114, 115, 116, and 117) according to the instructions enclosed in the kit. The labeled samples were acidified, mixed, and then desalted using  $\text{C}_{18}$  tips.<sup>28</sup> The eluted samples were dried by SpeedVac for mass spectrometry analysis.

### NanoLC–MS/MS and Data Analysis

The tryptic digests of exosomes ( $\sim 1.2 \mu\text{g}$ ) were separated on an EASY-nLC 1000 liquid chromatograph system (Thermo Fisher Scientific, San Jose, CA) with a 250 mm reverse-phase (RP)  $\text{C}_{18}$  column. The samples were eluted under a 120 min linear gradient from 2 to 35% acetonitrile in 0.1% formic acid at a constant flow rate of 300 nL/min.

An Orbitrap Fusion mass spectrometer (Thermo Fisher Scientific, San Jose, CA) operated in positive ion mode was employed for sample analysis. The capillary temperature and the spray voltage were set as 200 °C and 2.5 kV. The data were acquired in a data-dependent mode; the 15 strongest MS1 peaks were selected for subsequent MS2 analysis. For every selected peak, higher energy collisional dissociation (HCD) was performed. The MS1 spectra ( $m/z$  350–1650) and the MS2 spectra were both acquired in the Orbitrap.

The raw data were searched against the protein database by Proteome Discoverer 1.4 software (Thermo Fisher Scientific, San Jose, CA) with SEQUEST as the search engine. The parameters were set as follows: database: human UniProt; enzyme: trypsin; fixed modifications: carbamidomethyl (C) and 4-plex iTRAQ (N-term and K); variable modification: oxidation (M); up to two missed cleavages allowed; mass tolerance: 10 ppm for MS1 and mass tag, 0.05 Da for MS2; 1% false discovery rate allowed for peptides.

We normalized the quantification results manually to eliminate the difference of protein amounts from different time points (three time points of the patient serum and standard serum). The database search results were exported to Excel files. In each file, there was a column of the protein list and three columns of ratios 115/114, 116/114, and 117/114. All of these ratio values were  $\log_2$ -transformed. We calculated the mean of  $\log_2$  ratio values in each column and then subtracted this mean from every  $\log_2$  ratio value in this column. Thus the mean of the modified  $\log_2$  ratio values in each column was zero, which meant every time point (T2, T3, or T0) had been normalized with T1. Next, proteins with normalized  $\log_2$

ratio values from all files (patients) were combined. We performed a *t* test to filter out proteins with a large variation of expression level among different patients, such as low-abundance proteins, which were only identified in some patients. We eliminated the quantitative results of proteins that were not detected in more than half of the patients to increase the reliability of the results. The mean of the normalized  $\log_2$  ratio values from all patients was calculated for every protein. A protein was considered significantly changed if it had a normalized ratio  $>1.5$  (or  $<0.67$ ), where a normalized  $\log_2$  ratio was  $>0.585$  or  $<-0.585$ , with *p* value  $<0.05$ .

### Migration Assay

MiaPaCa-2 and Panc-1 cells were grown to 80% confluence in DMEM (Invitrogen, Waltham, MA) supplemented with 1% L-glutamine and 10% FBS at 37 °C and 5% CO<sub>2</sub> in six-well dishes. Three wounds per well were induced using a 200  $\mu$ L pipet tip. Growth medium was then changed to migration media (DMEM supplemented with 1% L-glutamine and 5% FBS). Serum derived from five healthy controls or four patients with locally advanced pancreatic cancer was added at a concentration of 5% to investigate the potential of serum-borne cancer-associated exosomes. Migration was observed at 0, 12, and 24 h after wound induction.

## Results

### Sample Preparation for Mass Spectrometry Analysis

The workflow started from the isolation of exosomes from patient serum is shown in Figure 1. Here we lysed exosomes, followed by sample preparation and protein digestion using the filter-aided sample preparation (FASP) method.<sup>29</sup> Peptide samples from different time points were labeled with iTRAQ tags and mixed for LC-MS/MS analysis. Exosome markers CD9, CD63, CD81, and TSG101 (Supplemental Figure S1a–d) were all observed in the list of proteins identified. We further selected CD63 antibody to perform Western blot and verified the result of mass spectrometry (Supplemental Figure S2).

### Specific Quantification of Total Exosomal Protein

To optimize the detection and quantification of exosomal cargo, we first had to address the problem of serum protein contamination in the purified exosome samples. Samples of various time points suffer from different levels of contamination, such as IgG fragments and fibronectin (FN), which are difficult to remove. The routine protein measuring method (e.g., the use of BCA protein measuring kit) determined the amount of total protein (exosome protein plus contamination protein), where the amounts of exosome protein were still uncertain (Figure 2a).

To solve this issue, we tested 10% of each tag-labeled sample using LC-MS/MS before mixing and obtained the amount of exosome protein by a label-free method. High-abundance contamination proteins including all forms of IgG and FN were deleted from the list of identified proteins. The remaining proteins were assumed to be derived from exosomes. Then, all peptide intensities of exosome proteins were  $\log_2$ -transferred, and their mean concentration was determined. The mean of  $\log_2$ -transferred peptide intensities

reflected the relative amount of exosome proteins (Supplemental Figure S3). The difference of means between samples of two time points was the  $\log_2$ -transferred ratio of their protein amount. According to these differences of means, we could mix the exosome protein samples of various time points at the ratio we expected (Figure 2b). Our optimized method compensates for differences in protein input due to serum protein contamination and thus allows for the quantification of exosomal cargo proteins and the direct comparison of different time points or patients.

### Optimized iTRAQ Labeling Procedure for the Detection of Low Amounts of Protein

To overcome the mass-spectrometry detection limit of low amounts of protein in the exosomal lysates, we aimed to establish an iTRAQ method that is able to compensate for the low amounts of clinically available serum samples without compromising protein detection. According to our experience, 1 to 2  $\mu\text{g}$  is the optimal amount for general nanoLC-MS/MS. However, we could only acquire 0.1 to 0.2  $\mu\text{g}$  exosome proteins from 4 mL of serum.

We designed an experiment, where we started with 36 mL of standard serum. After the exosome extraction and protein digestion, we split up the sample into nine aliquots (three aliquots for sample A and six aliquots for sample B). For sample A, each aliquot of exosome protein was labeled with an iTRAQ tag 114, 115, and 116, respectively, and then mixed together (Figure 2c). For sample B, each of three aliquots of exosome protein was labeled with iTRAQ-tags 114, 115, and 116, respectively, and the other three aliquots of exosome protein were labeled with an iTRAQ-tag 117. Samples A and B were analyzed separately by LC-MS/MS.

As a result, an average of 502 proteins were identified per run in sample A, among which 495 proteins were quantified. In sample B, an average of 603 proteins were identified per run, among which 562 proteins were quantified (Figure 2d). Here only proteins with all iTRAQ-tags detected were defined as being quantified. For the Samples A and B, the intensities of tags 114, 115, and 116 were identical, but 13.5% more proteins were quantified in the Sample B. The proteins exclusively quantified in sample B can be attributed to the higher intensities of parent ions and resulting fragment ions (e.g., b ion series and y ion series). Thus increasing the amount of either iTRAQ tag-labeled peptide would enhance the intensity of their common parent and fragment ions and further improve the peptide/protein identification efficiency.

Because the exosomes from healthy control and from patient serum share similar proteome profiles, this finding demonstrates that increasing the amount of healthy control (which is readily available) increases the common ion intensities of healthy control and patient serum and thereby increases the number of detected proteins in patient serum. This optimization is essential for the further development of clinical work flow, where the amount of available patient serum is limited.

### Exosomal Cargo of Patients with Locally Advanced Pancreatic Cancer

Using the iTRAQ labeling technique described above, we identified and quantified exosome proteins from the serum of 10 patients with locally advanced pancreatic cancer. In total, 1630 proteins were identified, among which 1559 proteins (700–800 proteins per patient)

were quantified (Supplemental Figure S4). Proteins without quantification information were <5% of total proteins identified. For these quantified proteins, 1424 proteins had Gene Ontology information. Proteins from the cytoplasm, plasma membrane, extracellular space, and nucleus account for 41.85, 23.10, 19.80, and 10.11%, respectively (Figure 3a). The functional analysis (Figure 3b) shows that those proteins are mainly enzyme (20.33%). There are also transporter (9.07%), peptidase (7.44%), kinase (4.04%), transmembrane receptor (3.82%), and regulator (3.54%) proteins. The pathway analysis (Figure 3c) shows that proteins involved in the immune response (33.24%), thrombosis (12.24%), metastasis (21.47%), and proliferation (7.06%) were enriched in our data set. Additionally, we detected proteins involved in vesicle trafficking (1.47%), cell death (4.71%), proteasomal degradation (4.12%), and cell stress (2.06%).

### **Tumor-Derived Exosomes Increase the Migration Potential of Pancreatic Cancer Cell Lines**

Because metastasis is a major obstacle in the successful treatment of pancreatic cancer patients and proteins involved in tumor metastasis are prominent in our data set (Supplemental Table S1, Figure 3c), we investigated the importance of tumor-derived exosomes for cell migration. To investigate the importance of pro-migratory proteins in the exosomes, Panc-1 and MiaPaCa2 cells were exposed to serum derived from healthy controls or patients. While the serum of healthy controls had little impact on cell migration in a wound-healing assay, faster wound closure was observed in cells exposed to serum derived from three out of four patients (Figures 4a, b). Although the total change in migration potential was significantly higher in Panc-1 cells, a similar trend was observed in MiaPaCa2 cells.

We further examined whether the increase in migration potential is conferred through soluble factors in the serum or proteins packed into exosomes. Treatment with exosome-depleted serum did not impact wound closure in either cell line (Figure 4c,e). Treatment with purified exosomes on the other hand resulted in an increase in migration similar to what was observed in response to treatment with full serum (Figure 4b,d,f).

### **Treatment-Induced Changes in Exosome Content**

We further evaluated changes in exosomal cargo in response to treatment with chemoradiotherapy. We analyzed exosomes before treatment (T1), after one cycle of induction gemcitabine based chemotherapy (T2), and at 3 weeks after starting chemoradiation therapy (T3) and compared these samples to serum derived from healthy volunteers (T0). We identified eight proteins that changed during a course of therapy in all patients. Transferrin receptor protein 1 (CD71) and lysozyme C (LYSC) have been shown to be involved in the regulation of proliferation, obscurin-like protein 1 (OBSL1) and vimentin in epithelial-to-mesenchymal-transition (EMT), platelet factor 4 (PLF4) in thrombosis, beta-parvin (PARVB), and microtubule-associated protein RP/EB family member 2 (MARE2) in cell motility, and HLA class I histocompatibility antigen B-51 alpha chain (1B51) in immune response.

In response to chemotherapy (T2), we found that 1B51, vimentin, and LYSC were down-regulated, while CD71, MARE2, PARVB, PLF4 (Supplemental Figure S1e), and OBSL1



(Supplemental Figure S1f) were up-regulated (Figure 5). Treatment with chemoradiation (T3) resulted in increased levels of 1B51, vimentin, and OBSL1 when compared with T2 and decreased levels of MARE2, LYSC, PLF4, CD71, and PARVB (Table 1).

Next, we compared the exosome proteins from T1 with those from healthy serum (T0), and found that 99 proteins were differentially expressed with 50 down-regulated and 49 up-regulated in T0 (Table 2). With the exception of vimentin and CD71, all of the common proteins showed higher expression levels in patients when compared with healthy control. While CD71 expression was higher in normal controls, no difference was observed in vimentin expression between patients at baseline (T1) and healthy controls.

## Discussion

Monitoring of treatment response in pancreatic cancer patients is hampered by the lack of reliable blood based biomarkers and the limited feasibility of performing serial biopsies. Tumor-derived exosomes have recently moved into the clinical focus in many different cancer types due to their availability as a part of routine blood draws, where the exosomal cargo can provide “snap shots” of cancer protein expression profiles and for their role in cell-to-cell communication.<sup>15,16</sup> The evaluation of tumor-derived exosomes, however, is limited by current mass spectrometry techniques.<sup>25,26</sup> Herein we report on a novel adaptation of the iTRAQ method that is able to overcome current limitations in protein detection and quantification. To deal with the issue of plasma-derived protein contamination, we designed a protein quantification method that allows the specific quantification of exosome-derived proteins and thus quantitatively compares the exosomal cargo of different patients. Furthermore, we adapted the iTRAQ method to increase detection sensitivity and allow the detection of low abundance proteins from low amounts of patient serum. To achieve this enhanced performance, we increased the amount of sample used from the healthy control. We labeled a detectable amount of commercial standard proteins of interest using one iTRAQ tag and mixed this with experimental samples labeled by other tags. The result was that we were able to quantify more proteins in patients including some that had not been previously detected due to their low levels in patient-derived exosomes.

Recent reports demonstrate that exosomes play an important role in the communication of tumor cells with the adjacent and systemic microenvironment and are important in the metastatic process.<sup>8,9,15,17,26,30–34</sup> A study by Costa-Silva et al. showed that pancreatic cancer exosomes are critical components of the metastatic cascade through their premetastatic niche formation in the liver and that the expression of specific integrins is responsible for the organotropism of metastasis that may allow for the prediction of metastatic potential and organotrophic character of a tumor.<sup>8,9</sup>

We found a number of proteins that were previously associated with tumor-derived exosomes, such as cyclins, integrins, and heat shock proteins.<sup>9,26,32</sup> Additionally, we detected a high number of proteins involved in EMT and metastasis, further supporting previous observations that tumor-derived exosomes play a crucial role in the development of metastasis.<sup>8,17,26,33,34</sup> These proteins were especially enriched when we evaluated changes in exosomal cargo over the course of a cycle of chemoradiation treatment. Unsurprisingly,

exosomal packing of these proteins is impacted by systemic treatment with chemotherapy as well as local treatment with radiation. We found eight proteins that displayed global treatment-induced changes in exosomal packaging that may reflect changes of expression levels in the releasing tumor cells. These changes appear to be specific to the treatment modality rather than treatment response or patient outcome. We cannot for certain claim that these proteins originate from exosomes from the pancreas because all organs secrete exosomes. However, given that there are proteins that are related to EMT and metastasis detected and that some of these change in a consistent manner with treatment, it is likely that they indeed originate from exosomes from the pancreas. Also, in our study, patient-derived exosomes significantly increased the migration potential of pancreatic cancer cells.

While we were able to evaluate the impact of tumor-derived exosomes of four patients on migration, the availability of limited amounts of patient serum prevented us from evaluating the same patients' samples by mass spectrometry and in migrations assays. Therefore, it is not possible to make a direct comparison between the detected proteins and changes in migration potential. Future prospective studies collecting higher volumes of blood samples in a larger patient population will be needed to address this issue.

## Conclusions

Our results further support the importance of tumor-derived exosomes in cancer progression and metastasis, although further studies are necessary to identify key proteins and unveil potential therapeutic targets. The optimized iTRAQ method may provide a clinically available method to monitor treatment response and classify pancreatic cancer patients based on exosome content. This method also has a wider application, where it can improve the mass-spectrometry detection limit of low-abundance proteins. Among a total of 1559 proteins quantified, 8 proteins show global treatment-specific changes in all of the patients and may be potential biomarkers of treatment response or metastasis for pancreatic cancer. Two of these, namely, OBSL1 and PLF4 display the highest treatment response in our data set, and we believe that the proteins are strong candidates for biomarker development.

## Supplementary Material

Refer to Web version on PubMed Central for supplementary material.

## Acknowledgments

This work is supported by the National Institutes of Health under grant R01GM49500 (D.M.L.) and the National Cancer Institute under grants RO1CA163895 (M.A.M.), P5OCA130810 (M.A.M., T.S.L.) and R21CA189775 (D.M.L.). We acknowledge the assistance of the Wayne State University Proteomics Core that is supported through National Institutes of Health grants P30 ES020957, P30 CA 022453, and S10 OD010700.

## References

1. American Cancer Society. Cancer Facts & Figures 2017. Atlanta: American Cancer Society; 2017. p. 3
2. Hammel P, Huguet F, van Laethem JL, Goldstein D, Glimelius B, Artru P, Borbath I, Bouche O, Shannon J, Andre T, Mineur L, Chibaudel B, Bonnetain F, Louvet C. Effect of Chemoradiotherapy vs Chemotherapy on Survival in Patients With Locally Advanced Pancreatic Cancer Controlled

After 4 Months of Gemcitabine With or Without Erlotinib: The LAP07 Randomized Clinical Trial. *JAMA*. 2016; 315:1844–1853. [PubMed: 27139057]

3. Sawicka E, Mironczuk A, Wojtukiewicz MZ, Sierko E. Chemoradiotherapy for locally advanced pancreatic cancer patients: is it still an open question? *Wspolczesna Onkol*. 2016; 2:102–108.
4. Herreros-Villanueva M, Bujanda L. Non-invasive biomarkers in pancreatic cancer diagnosis: what we need versus what we have. *Ann Transl Med*. 2016; 4:134. [PubMed: 27162784]
5. Xia J, Chen C, Chen Z, Miele L, Sarkar FH, Wang Z. Targeting pancreatic cancer stem cells for cancer therapy. *Biochim Biophys Acta, Rev Cancer*. 2012; 1826:385–399.
6. Li C, Wu JJ, Hynes M, Dosch J, Sarkar B, Welling TH, Pasca di Magliano M, Simeone DM. c-Met is a marker of pancreatic cancer stem cells and therapeutic target. *Gastroenterology*. 2011; 141:2218–2227. [PubMed: 21864475]
7. Gallo A, Tandon M, Alevizos I, Illei GG. The majority of microRNAs detectable in serum and saliva is concentrated in exosomes. *PLoS One*. 2012; 7:e30679. [PubMed: 22427800]
8. Costa-Silva B, Aiello NM, Ocean AJ, Singh S, Zhang H, Thakur BK, Becker A, Hoshino A, Mark MT, Molina H, Xiang J, Zhang T, Theilen TM, Garcia-Santos G, Williams C, Ararso Y, Huang Y, Rodrigues G, Shen TL, Labori KJ, Lothe IM, Kure EH, Hernandez J, Doussot A, Ebbesen SH, Grandgenett PM, Hollingsworth MA, Jain M, Mallya K, Batra SK, Jarnagin WR, Schwartz RE, Matei I, Peinado H, Stanger BZ, Bromberg J, Lyden D. Pancreatic cancer exosomes initiate pre-metastatic niche formation in the liver. *Nat Cell Biol*. 2015; 17:816–826. [PubMed: 25985394]
9. Hoshino A, Costa-Silva B, Shen TL, Rodrigues G, Hashimoto A, Tesic Mark M, Molina H, Kohsaka S, Di Giannatale A, Ceder S, Singh S, Williams C, Sopolop N, Uryu K, Pharmer L, King T, Bojmar L, Davies AE, Ararso Y, Zhang T, Zhang H, Hernandez J, Weiss JM, Dumont-Cole VD, Kramer K, Wexler LH, Narendran A, Schwartz GK, Healey JH, Sandstrom P, Labori KJ, Kure EH, Grandgenett PM, Hollingsworth MA, de Sousa M, Kaur S, Jain M, Mallya K, Batra SK, Jarnagin WR, Brady MS, Fodstad O, Muller V, Pantel K, Minn AJ, Bissell MJ, Garcia BA, Kang Y, Rajasekhar VK, Ghajar CM, Matei I, Peinado H, Bromberg J, Lyden D. Tumour exosome integrins determine organotropic metastasis. *Nature*. 2015; 527:329–335. [PubMed: 26524530]
10. Simpson RJ, Jensen SS, Lim JW. Proteomic profiling of exosomes: current perspectives. *Proteomics*. 2008; 8:4083–4099. [PubMed: 18780348]
11. Shao H, Chung J, Balaj L, Charest A, Bigner DD, Carter BS, Hochberg FH, Breakefield XO, Weissleder R, Lee H. Protein typing of circulating microvesicles allows real-time monitoring of glioblastoma therapy. *Nat Med*. 2012; 18:1835–1840. [PubMed: 23142818]
12. Wu H, Zhou J, Mei S, Wu D, Mu Z, Chen B, Xie Y, Ye Y, Liu J. Circulating exosomal microRNA-96 promotes cell proliferation, migration and drug resistance by targeting LMO7. *J Cell Mol Med*. 2016; doi: 10.1111/jcmm.13056
13. Al-Hajj M, Wicha MS, Benito-Hernandez A, Morrison SJ, Clarke MF. Prospective identification of tumorigenic breast cancer cells. *Proc Natl Acad Sci U S A*. 2003; 100:3983–3988. [PubMed: 12629218]
14. van den Boorn JG, Dassler J, Coch C, Schlee M, Hartmann G. Exosomes as nucleic acid nanocarriers. *Adv Drug Delivery Rev*. 2013; 65:331–335.
15. Yang C, Robbins PD. The roles of tumor-derived exosomes in cancer pathogenesis. *Clin Dev Immunol*. 2011; 2011:842849. [PubMed: 22190973]
16. Vlassov AV, Magdaleno S, Setterquist R, Conrad R. Exosomes: current knowledge of their composition, biological functions, and diagnostic and therapeutic potentials. *Biochim Biophys Acta, Gen Subj*. 2012; 1820:940–948.
17. Hood JL, San RS, Wickline SA. Exosomes released by melanoma cells prepare sentinel lymph nodes for tumor metastasis. *Cancer Res*. 2011; 71:3792–3801. [PubMed: 21478294]
18. Simpson RJ, Lim JW, Moritz RL, Mathivanan S. Exosomes: proteomic insights and diagnostic potential. *Expert Rev Proteomics*. 2009; 6:267–283. [PubMed: 19489699]
19. Gonzales PA, Pisitkun T, Hoffert JD, Tchapyjnikov D, Star RA, Kleta R, Wang NS, Knepper MA. Large-scale proteomics and phosphoproteomics of urinary exosomes. *J Am Soc Nephrol*. 2009; 20:363–379. [PubMed: 19056867]

20. Chen Y, Xie Y, Xu L, Zhan S, Xiao Y, Gao Y, Wu B, Ge W. Protein content and functional characteristics of serum-purified exosomes from patients with colorectal cancer revealed by quantitative proteomics. *Int J Cancer*. 2017; 140:900–913. [PubMed: 27813080]
21. Clark DJ, Fondrie WE, Liao Z, Hanson PI, Fulton A, Mao L, Yang AJ. Redefining the Breast Cancer Exosome Proteome by Tandem Mass Tag Quantitative Proteomics and Multivariate Cluster Analysis. *Anal Chem*. 2015; 87:10462–10469. [PubMed: 26378940]
22. Zhao X, Wu Y, Duan J, Ma Y, Shen Z, Wei L, Cui X, Zhang J, Xie Y, Liu J. Quantitative proteomic analysis of exosome protein content changes induced by hepatitis B virus in Huh-7 cells using SILAC labeling and LC-MS/MS. *J Proteome Res*. 2014; 13:5391–5402. [PubMed: 25265333]
23. Lasser C, O'Neil SE, Shelke GV, Sihlbom C, Hansson SF, Gho YS, Lundback B, Lotvall J. Exosomes in the nose induce immune cell trafficking and harbour an altered protein cargo in chronic airway inflammation. *J Transl Med*. 2016; 14:181. [PubMed: 27320496]
24. Rodriguez-Suarez E, Gonzalez E, Hughes C, Conde-Vancells J, Rudella A, Royo F, Palomo L, Elortza F, Lu SC, Mato JM, Vissers JP, Falcon-Perez JM. Quantitative proteomic analysis of hepatocyte-secreted extracellular vesicles reveals candidate markers for liver toxicity. *J Proteomics*. 2014; 103:227–240. [PubMed: 24747303]
25. Minciacchi VR, You S, Spinelli C, Morley S, Zandian M, Aspuria PJ, Cavallini L, Ciardiello C, Reis Sobreiro M, Morello M, Kharmate G, Jang SC, Kim DK, Hosseini-Beheshti E, Tomlinson Guns E, Gleave M, Gho YS, Mathivanan S, Yang W, Freeman MR, Di Vizio D. Large oncosomes contain distinct protein cargo and represent a separate functional class of tumor-derived extracellular vesicles. *Oncotarget*. 2015; 6:11327–11341. [PubMed: 25857301]
26. Campanella C, Bavisotto C, Gammazza A, Nikolic D, Rappa F, David S, Cappello F, Bucchieri F, Fais S. Exosomal Heat Shock Proteins as New Players in Tumour Cell-to-Cell Communication. *Journal of Circulating Biomarkers*. 2014; 3:4.
27. Kim J, Tan Z, Lubman DM. Exosome enrichment of human serum using multiple cycles of centrifugation. *Electrophoresis*. 2015; 36:2017–2026. [PubMed: 26010067]
28. An M, Zou X, Wang Q, Zhao X, Wu J, Xu LM, Shen HY, Xiao X, He D, Ji J. High-confidence de novo peptide sequencing using positive charge derivatization and tandem MS spectra merging. *Anal Chem*. 2013; 85:4530–4537. [PubMed: 23536960]
29. Wisniewski JR, Zougman A, Nagaraj N, Mann M. Universal sample preparation method for proteome analysis. *Nat Methods*. 2009; 6:359–362. [PubMed: 19377485]
30. Jeppesen DK, Nawrocki A, Jensen SG, Thorsen K, Whitehead B, Howard KA, Dyrskjot L, Orntoft TF, Larsen MR, Ostfeld MS. Quantitative proteomics of fractionated membrane and lumen exosome proteins from isogenic metastatic and non-metastatic bladder cancer cells reveal differential expression of EMT factors. *Proteomics*. 2014; 14:699–712. [PubMed: 24376083]
31. Ramteke A, Ting H, Agarwal C, Mateen S, Somasagara R, Hussain A, Graner M, Frederick B, Agarwal R, Deep G. Exosomes secreted under hypoxia enhance invasiveness and stemness of prostate cancer cells by targeting adherens junction molecules. *Mol Carcinog*. 2015; 54:554–565. [PubMed: 24347249]
32. Munson P, Shukla A. Exosomes: Potential in Cancer Diagnosis and Therapy. *Medicines (Basel)*. 2015; 2:310–327. [PubMed: 27088079]
33. Grange C, Tapparo M, Collino F, Vitillo L, Damasco C, Deregibus MC, Tetta C, Bussolati B, Camussi G. Microvesicles released from human renal cancer stem cells stimulate angiogenesis and formation of lung premetastatic niche. *Cancer Res*. 2011; 71:5346–5356. [PubMed: 21670082]
34. Koumangoye RB, Sakwe AM, Goodwin JS, Patel T, Ochieng J. Detachment of breast tumor cells induces rapid secretion of exosomes which subsequently mediate cellular adhesion and spreading. *PLoS One*. 2011; 6:e24234. [PubMed: 21915303]

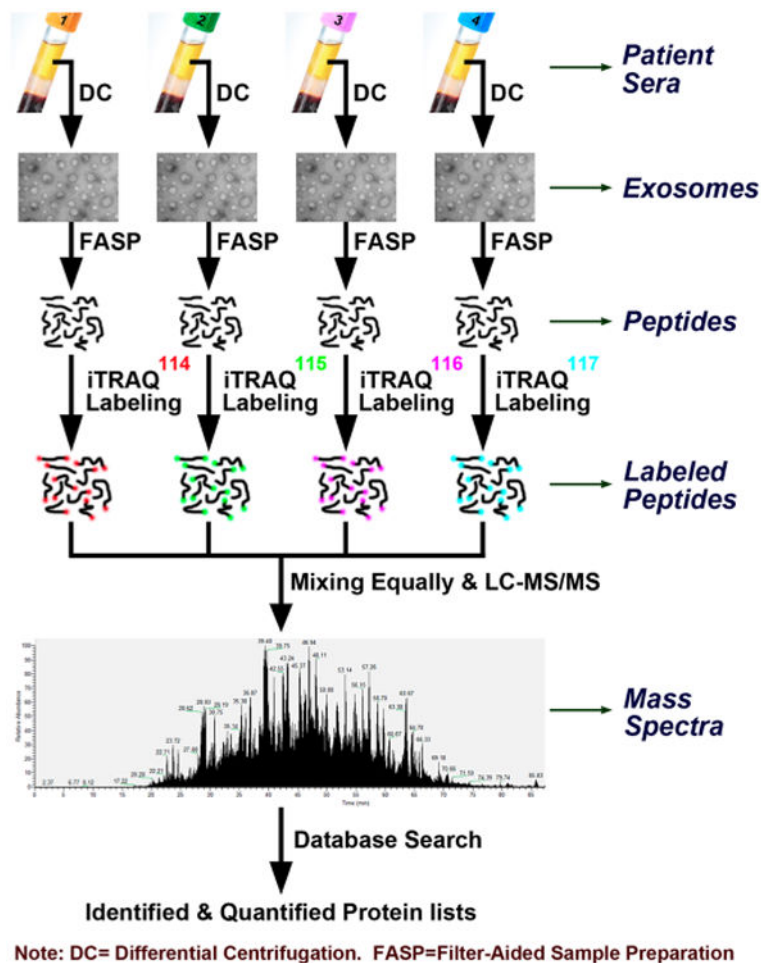


**Figure 1.**

Workflow of mass spectrometry identification and quantitation of exosome proteins from patient serum. Schematic overview of the sample preparation and LC–MS/MS analysis of patient and control serum samples. Exosomes were isolated from sera of patients with pancreatic cancer using several steps of differential centrifugation. Then, proteins were extracted, alkylated, and digested in ultracentrifugal tubes using the filter-aided sample preparation (FASP) method. Next, peptides were labeled with isobaric tags for relative and absolute quantitation (iTRAQ). Next, all plex of iTRAQ-labeled peptides were mixed and run on a mass spectrometer. Finally, database search of raw data and statistical analysis identified the differentially expressed proteins.

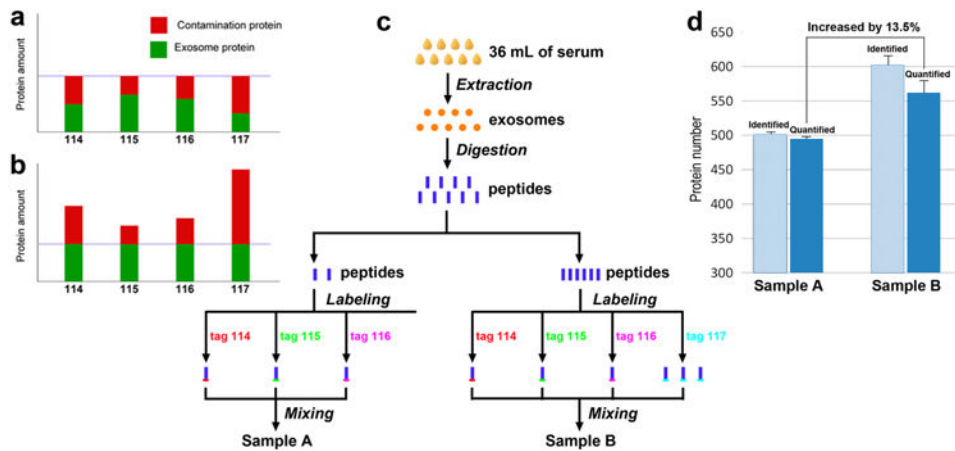


**Figure 2.**

Optimization of the iTRAQ method significantly improved the quantification of tumor-derived exosomal proteins. (a) Routine protein measuring method determined the amounts of total protein (exosome protein plus contamination protein), where the amounts of exosome protein were still uncertain. To compensate for this, (b) we used a label-free method to determine the exosome content of each tag-labeled sample before mixing. The x axis and y axis labels (a and b) represent sample labeled by four different iTRAQ mass tags (114, 115, 116, or 117) and relative protein amount of every sample, respectively. (c) Initially 36 mL of standard serum was used to extract exosomes and obtain protein. In sample A, each aliquot of exosome protein was labeled by tag 114, 115, and 116, respectively. In sample B, the situation was similar, except the other three aliquots of exosome protein were labeled tag 117. (d) An average of 502 proteins were identified in sample A and 495 proteins were quantified, while an average of 603 proteins were identified in sample B and 562 proteins were quantified. For both samples, the intensities of tags 114, 115, and 116 were identical; but 13.5% more proteins were quantified in the Sample B.

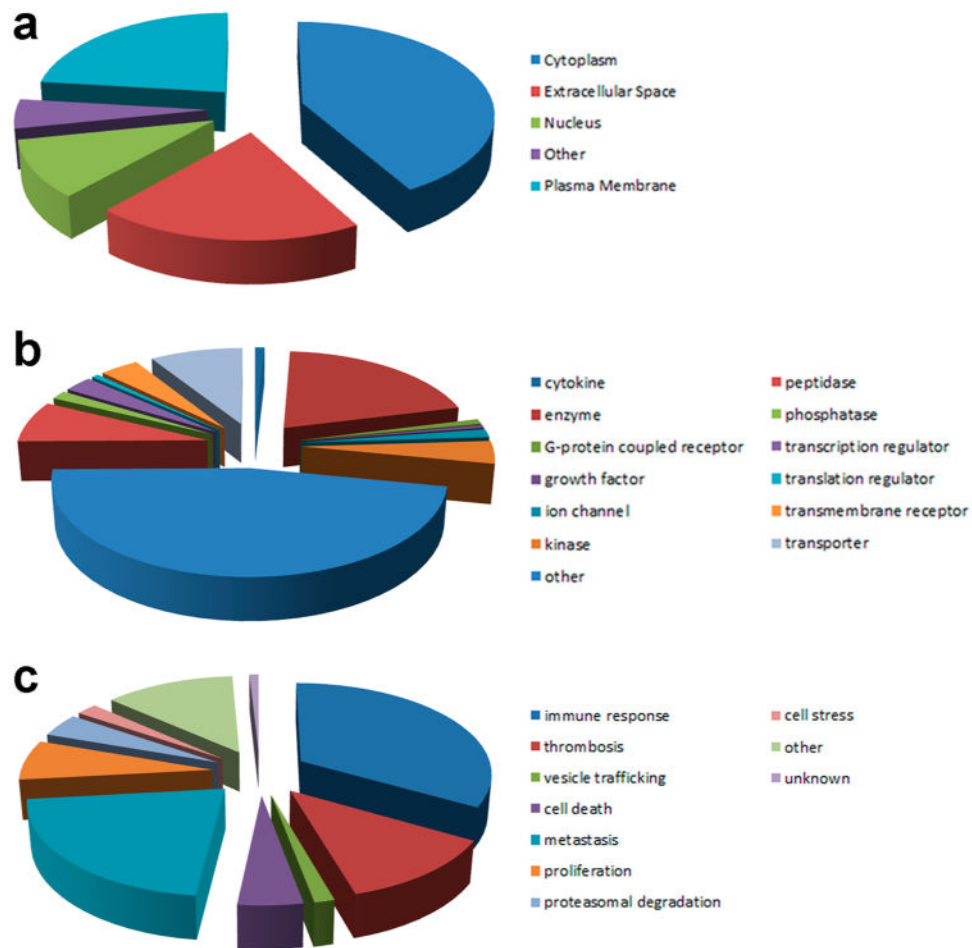


**Figure 3.** Analysis of exosomal protein content. Among 1559 quantified proteins, 1424 proteins had GO information. (a) The subcellular distribution shows that proteins from cytoplasm, plasma membrane, extracellular space, and nucleus account for 41.85, 23.10, 19.80, and 10.11%, respectively. (b) The functional analysis shows that those proteins are mainly enzyme (20.33%), transporter (9.07%), peptidase (7.44%), kinase (4.04%), transmembrane receptor (3.82%), and regulator (3.54%). (c) The pathway analysis shows that proteins involved in the immune response (33.24%), thrombosis (12.24%), metastasis (21.47%), and proliferation (7.06%) were enriched in our data set.

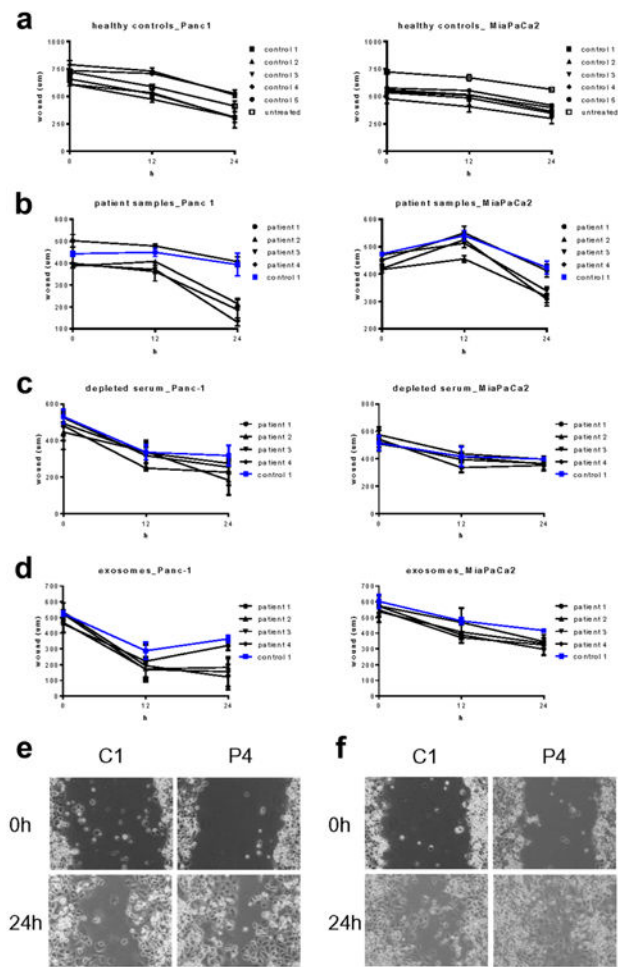


**Figure 4.**

Tumor-derived exosomes increase the migration potential of pancreatic cancer cell lines. To evaluate changes in migration potential, Panc-1 and MiaPaCa2 cells were exposed to the (a) serum of 5 healthy controls, (b) the serum of four patients with locally advanced pancreatic cancer, (c) exosome-depleted serum, or (d) purified exosomes in a wound healing assay. Wound closure was evaluated 0, 12, and 24 h after wound induction. While treatment with (a) serum derived from healthy controls had no impact on migration in either cell line, (b) the migration potential was increased in cells treated with serum from patients 2, 3, and 4 but not patient 1. (c) Depletion of exosomes from patient serum negated the pro-migratory effects of patient serum. (d) Pro-migratory effects of patient serum can be attributed to serum exosomes and are preserved in purified exosomes. Representative images of Panc-1 cells treated with (e) exosome-depleted serum or (f) purified exosomes of a healthy control and a patient with locally advanced pancreatic cancer. Error bars represent SD ( $n = 3$ ).



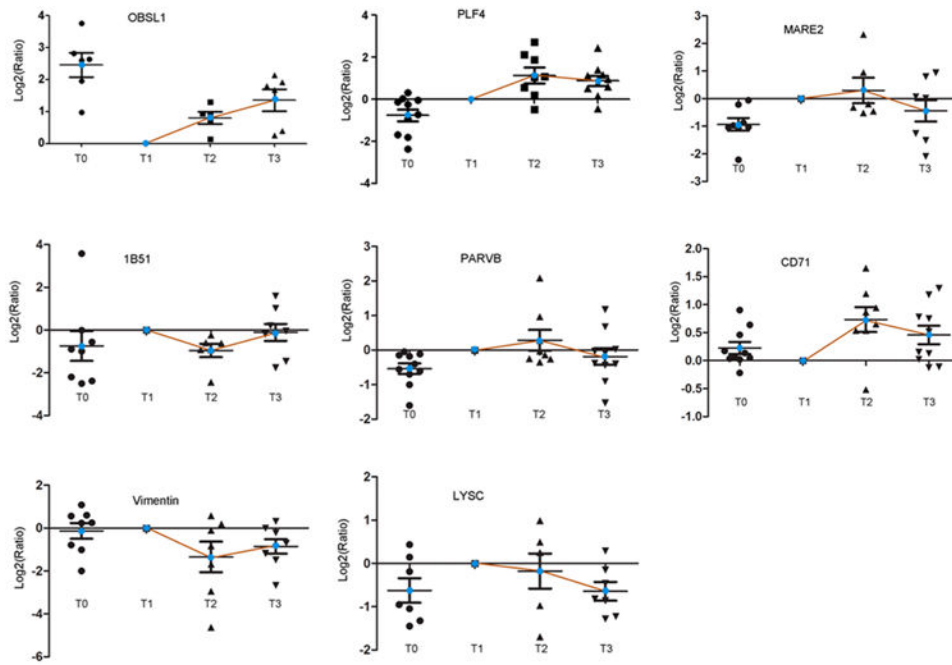


**Figure 5.** Changes in exosomal cargo in response to treatment with chemoradiotherapy. Treatment-induced changes in the expression of (a) OBSL1, (b) PLF4, (c) MARE2, (d) 1B51, (e) PARVB, (f) CD71, (g) vimentin, and (h) LYSC. Protein expression was evaluated in exosomes derived from healthy controls (T0) and patients prior to treatment (T1), after chemotherapy (T2) and at the midpoint of a cycle of chemoradiotherapy (T3).

Table 1

Differentially Expressed Exosomal Proteins during Treatments<sup>a</sup>

Accession	Abbreviation	<i>p</i>	Mean	<i>p</i>	Mean	<i>p</i>	Mean	<i>p</i>	Mean
			normalized log <sub>2</sub> (T2/T1)		normalized log <sub>2</sub> (T3/T1)		normalized log <sub>2</sub> (T3/T2)		normalized log <sub>2</sub> (T0/T1)
P02786	CD71	<i>0.013</i>	<b>0.733</b>	<i>0.022</i>	0.458	<i>0.107</i>	-0.351	<i>0.063</i>	0.227
O75147	OBSL1	<i>0.017</i>	<b>0.800</b>	<i>0.010</i>	<b>1.357</b>	<i>0.153</i>	0.494	<i>0.001</i>	<b>2.451</b>
P02776	PLF4	<i>0.020</i>	<b>1.125</b>	<i>0.007</i>	<b>0.853</b>	<i>0.752</i>	-0.141	<i>0.025</i>	<b>-0.769</b>
P18464	IB51	<i>0.020</i>	<b>-0.955</b>	<i>0.784</i>	-0.113	<i>0.116</i>	<b>0.600</b>	<i>0.321</i>	<b>-0.745</b>
P08670	Vimentin	<i>0.108</i>	<b>-1.346</b>	<i>0.039</i>	<b>-0.854</b>	<i>0.301</i>	0.497	<i>0.729</i>	-0.132
P61626	LYSC	<i>0.562</i>	-0.177	<i>0.025</i>	<b>-0.644</b>	<i>0.268</i>	-0.437	<i>0.069</i>	<b>-0.625</b>
Q9HBI1	PARVB	<i>0.367</i>	0.287	<i>0.449</i>	-0.189	<i>0.007</i>	<b>-0.660</b>	<i>0.007</i>	-0.536
Q15555	MARE2	<i>0.638</i>	0.296	<i>0.293</i>	-0.441	<i>0.004</i>	<b>-1.029</b>	<i>0.005</i>	<b>-0.932</b>

<sup>a</sup>Red and blue represent up-regulated and down-regulated, respectively. Green indicates *p* value <0.05. The mean is labeled in bold if its *p* value is <0.05.

**Table 2**  
**Differentially Expressed Proteins of Exosomes between Healthy Control (T0) and Patients with Pancreatic Cancer (T1)<sup>a</sup>**

Accession	Protein name	Abbreviation	normalized log <sub>2</sub> (T0/T1)	
			<i>p</i>	Mean
P80511	Protein S100-A12	S10AC	0.00366	-1.71055
Q5SZB4	Uncharacterized protein C9orf50	CI050	0.02523	-1.70237
P02679	Fibrinogen gamma chain	FIBG	0.00315	-1.25495
P02671	Fibrinogen alpha chain	FIBA	0.00135	-1.23430
O15145	Actin-related protein 2/3 complex subunit 3	ARPC3	0.00411	-1.08119
P68032	Actin, alpha cardiac muscle 1	ACTC	0.00874	-1.07614
P32119	Peroxiredoxin-2	PRDX2	0.00030	-0.97950
P00915	Carbonic anhydrase 1	CAH1	0.00048	-0.97735
O00187	Mannan-binding lectin serine protease 2	MASP2	0.00225	-0.95533
P00736	Complement C1r subcomponent	C1R	0.00222	-0.94732
Q15555	Microtubule-associated protein RP/EB family member 2	MARE2	0.00487	-0.93202
P12109	Collagen alpha-1(VI) chain	CO6A1	0.00163	-0.92449
P27918	Properdin	PROP	0.00001	-0.91328
P12259	Coagulation factor V	FA5	0.00002	-0.91248
Q15485	Ficolin-2	FCN2	0.00006	-0.89729
Q13201	Multimerin-1	MMRN1	0.00074	-0.85019
Q6E0U4	Dermokine	DMKN	0.02603	-0.82876
Q9H299	SH3 domain-binding glutamic acid-rich-like protein 3	SH3L3	0.00583	-0.81949
P09871	Complement C1s subcomponent	C1S	0.00411	-0.80813
P02763	Alpha-1-acid glycoprotein 1	A1AG1	0.01322	-0.80272
P02656	Apolipoprotein C-III	APOC3	0.00650	-0.79554
P08493	Matrix Gla protein	MGP	0.00572	-0.79406
O75636	Ficolin-3	FCN3	0.01612	-0.79155
Q8WWZ8	Oncoprotein-induced transcript 3 protein	OIT3	0.00095	-0.78631
Q4LDE5	Sushi, von Willebrand factor type A, EGF and pentraxin domain-containing protein 1	SVEP1	0.00778	-0.77352
P02675	Fibrinogen beta chain	FIBB	0.01183	-0.77158
P02776	Platelet factor 4	PLF4	0.02528	-0.76856
P02747	Complement C1q subcomponent subunit C	C1QC	0.04389	-0.76156
P60174	Triosephosphate isomerase	TPIS	0.00020	0.73316
Q15942	Zyxin	ZYX	0.00052	-0.73005
P61981	14-3-3 protein gamma	1433G	0.00713	-0.72367
P69905	Hemoglobin subunit alpha	HBA	0.00179	-0.72069
P01042	Kininogen-1	KNG1	0.00009	-0.71929
Q08830	Fibrinogen-like protein 1	FGL1	0.00959	-0.71273

Accession	Protein name	Abbreviation	normalized log <sub>2</sub> (T0/T1)	
			<i>p</i>	Mean
P68366	Tubulin alpha-4A chain	TBA4A	0.01286	-0.69262
P07195	L-lactate dehydrogenase B chain	LDHB	0.00495	-0.68326
P37802	Transgelin-2	TAGL2	0.00360	-0.67952
P08311	Cathepsin G	CATG	0.02429	-0.67802
Q16610	Extracellular matrix protein 1	ECM1	0.00921	-0.67386
P78509	Reelin	RELN	0.03549	-0.66996
P60709	Actin, cytoplasmic 1	ACTB	0.00067	-0.65437
O15143	Actin-related protein 2/3 complex subunit 1B	ARC1B	0.00387	-0.65172
P18085	ADP-ribosylation factor 4	ARF4	0.04294	-0.64543
P30041	Peroxiredoxin-6	PRDX6	0.00155	-0.63975
P00488	Coagulation factor XIII A chain	F13A	0.00252	-0.62313
P23528	Cofilin-1	COF1	0.00524	-0.61940
P68871	Hemoglobin subunit beta	HBB	0.00349	-0.61381
P63104	14-3-3 protein zeta/delta	1433Z	0.00360	-0.59736
P06727	Apolipoprotein A-IV	APOA4	0.04771	-0.58892
P59998	Actin-related protein 2/3 complex subunit 4	ARPC4	0.00270	-0.58543
P0CG48	Polyubiquitin-C	UBC	0.01690	0.58522
P27169	Serum paraoxanase/arylesterase 1	PON1	0.00033	0.59535
P01591	Immunoglobulin J chain	IGJ	0.02380	0.59850
P02787	Serotransferrin	TRFE	0.00051	0.62796
P11226	Mannose-binding protein C	MBL2	0.04009	0.66116
Q8IWA5	Cholin transporter-like protein 2	CTL2	0.00028	0.66591
Q8N699	Myc target protein 1	MYCT1	0.00010	0.66966
Q99829	Copine-1	CPNE1	0.00090	0.67289
P20851	C4b-binding protein beta chain	C4BPB	0.01293	0.67424
P00751	Complement factor B	CFAB	0.00465	0.67668
P48509	CD151 antigen	CD151	0.03383	0.69911
Q8NG11	Tetraspanin-14	TSN14	0.00002	0.70594
Q8WZ42	Titin	TITIN	0.04448	0.72817
Q96CX2	BTB/POZ domain-containing protein KCTD12	KCD12	0.00264	0.73408
P01009	Alpha-1-antitrypsin	A1AT	0.00012	0.74567
P00740	Coagulation factor IX	FA9	0.00041	0.74972
P02647	Apolipoprotein A-I	APOA1	0.00220	0.75035
P02652	Apolipoprotein A-II	APOA2	0.00600	0.79768
Q9UQP3	Tenascin N	TENN	0.00192	0.83012
Q6GTS8	Probable carboxypeptidase Mp20D1	P20D1	0.00026	0.84015
P22891	Vitamin K-dependent protein Z	PROZ	0.00652	0.84381
Q6UX06	Olfactomedin-4	OLFM4	0.00098	0.84697

Accession	Protein name	Abbreviation	normalized log <sub>2</sub> (T0/T1)	
			<i>p</i>	Mean
P21926	CD9 antigen	CD9	0.00087	0.85892
O14791	Apolipoprotein L1	APOL1	0.00022	0.89338
P28676	Grancalcin	GRAN	0.00012	0.89480
P09525	Annexin A4	ANXA4	0.00000	0.90554
P35858	Insulin-like growth factor-binding protein complex acid labile subunit	ALS	0.03731	0.91192
P01019	Angiotensinogen	ANGT	0.00008	0.92375
O75052	Carboxyl-terminal PDZ ligand of neuronal nitric oxide synthase protein	CAPON	0.04511	0.92664
P30626	Sorcin	SORCN	0.00005	0.96897
P00738	Haptoglobin	HPT	0.00000	0.98060
P50995	Annexin A11	ANX11	0.00000	1.00394
P17936	Insulin-like growth factor-binding protein 3	IBP3	0.00753	1.01661
P00748	Coagulation factor XII	FA12	0.01941	1.03233
O75340	Programmed cell death protein	PDCD6	0.00004	1.03303
Q5VU65	Nuclear pore membrane glycoprotein 210-like	P210L	0.01735	1.08934
P20073	Annexin A7	ANXA7	0.00000	1.12203
P08962	CD63 antigen	CD63	0.00047	1.15061
P04114	Apolipoprotein B-100	APOB	0.00042	1.17624
A6NJ16	Putative V-set and immunoglobulin domain-containing-like protein IGHV4OR15-8	IV4F8	0.01621	1.18668
P23069	Genome polyprotein	POLG	0.03860	1.19560
P00739	Haptoglobin-related protein	HPTR	0.00026	1.21999
P19652	Alpha-1-acid glycoprotein 2	A1AG2	0.00001	1.23090
P35542	Serum amyloid A-4 protein	SAA4	0.00382	1.28177
P00742	Coagulation factor X	FA10	0.00000	1.35757
P55056	Apolipoprotein C-IV	APOC4	0.00018	1.47476
Q65900	Genome polyprotein	POLG	0.03128	1.58371
Q13103	Secreted phosphoprotein 24	SPP24	0.00012	1.66737
O75147	Obscurin-like protein 1	OBSL1	0.00130	2.45142

<sup>a</sup>Compared with T1, 50 exosomal proteins were down-regulated and 49 were up-regulated in T0. Red and blue represent up-regulated and down-regulated, respectively.